

Sensitivity Analysis for a Space Debris Environment Model

Gian Luigi Somma*, Hugh G. Lewis**, and Camilla Colombo***

* *Faculty of Engineering and Environment, University of Southampton, United Kingdom, GL.Somma@soton.ac.uk*

** *Faculty of Engineering and Environment, University of Southampton, United Kingdom, H.G.Lewis@soton.ac.uk*

*** *Department of Aerospace Science and Technology, Politecnico di Milano, Italy, Camilla.Colombo@polimi.it*

Abstract

In space debris models, even a small change in the simulation variables can profoundly influence the evolution of the orbital population. The focus of this paper is to investigate the response of the LEO environment to the change in number and distribution of new object launched. The results of the performed sensitivity analysis suggest that the more critical regions lie in 800-1000 km and 1100-1300 km.

Keywords: space debris, modelling, sensitivity analysis, launch rate

1. Introduction

Space debris models are based on several critical hypothesis that can deeply influence the model behaviour and its results. Sometimes even a small change in the simulation variables (e.g. due to a different distribution, uncertainty or other factors) can lead to significant variations in the evolution of the orbital population. Moreover, some simulation variables have a significant uncertainty (e.g. the uncatalogued space debris population) or just cannot be predicted by their own nature of future event [1]. Some of these variables, mostly linked to physical parameters or behaviours, can be improved (at least partially) by increasing our knowledge on the subject, e.g. improving the solar and the atmospheric density models to enhance re-entry predictions or perform more observing campaign to increase the accuracy on the actual debris population. A second group of variables relates directly to the simulation hypothesis and are for example the future launch rate and their profile, the satellite operative life, the Post Mission Disposal (PMD) compliance level and the residual lifetime.

The aim of this paper is to investigate the influence of different launch rates and profiles in the Low Earth Orbit (LEO) in order to understand its effect on the evolution of the orbital population. The focus of an increasing launch rate is also of particular interest in light of the recent proposal by many private companies in the deployment of the so-called “mega constellations” [2,3]. Therefore, different launch rates and distributions may simulate the build-up and the replenishment of orbital constellations.

2. The model

The analysis presented in this paper are carried out using MISSD (Model to Investigate control Strategies for Space Debris), a source-sink statistical model for the LEO developed at University of Southampton [4,5].

2.1. Model description

MISSD is a multi-shell multi-species statistical source-sink model for LEO. It is based on a set of first order differential equation used to compute the object injection and removal from a custom number of evenly spaced circular altitude shells around the Earth, from 200 to 2000 km (see Section 2.2). The model accounts for six species: active payloads, inactive payloads, rocket bodies, mission-related objects (MROs), explosion fragments and collision fragments (Figure 1).

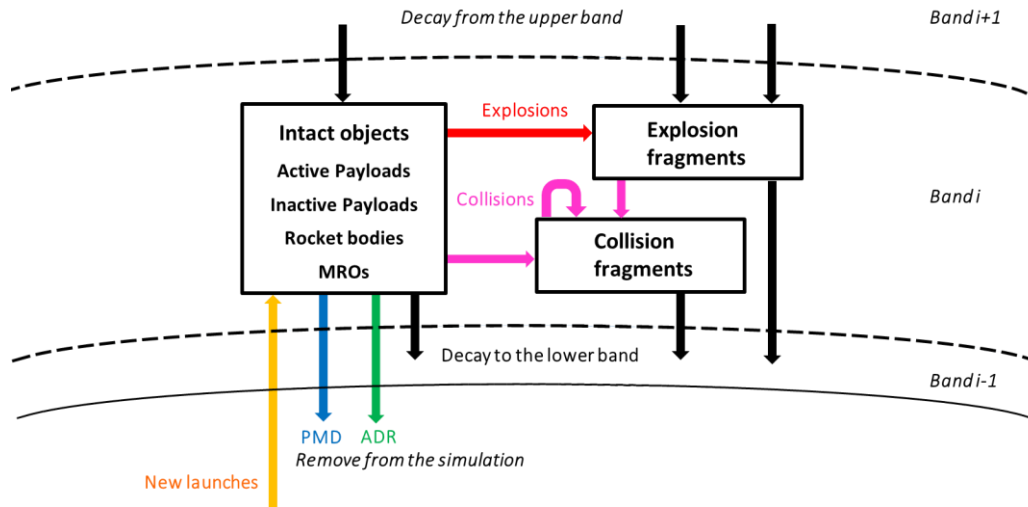


Figure 1: A simplified schematics of the model. Source and sink mechanisms are depicted as inbound and outbound arrows respectively. New objects are created with launches, explosions and collisions, while are removed via the natural drag, post-mission disposal, and active debris removal.

Each object species interact with each other via a collision matrix, while the four intact species can also generate fragments via explosions. The number of generated fragments for both collisions and explosions is computed via the standard break-up model [6,7]. Launches inject only active payloads, rocket bodies and MROs, while the only natural sink effect is the natural drag which is obtained from a piecewise exponential model of the Earth's density with an 11-year solar cycle [8,9]. Solar radiation pressure, Earth harmonics, and Luni-solar and other perturbations are not taken into account. Under the hypothesis that active satellites perform station-keeping manoeuvres, they remain in the same initial shell for all their operative time, after which they are moved into the inactive payload species. Post-mission disposal is implemented in a simplifying way, assuming that satellites are removed from the same shell accordingly to the past launch profile and a PMD compliance level parameter (from 0% to 100%). The model is also able to perform active debris removal (ADR) on inactive satellite and rocket bodies with either a constant value or an automatic proportional controller able to use different control laws [4]. An initial population file generates mean physical characteristics (area, mass, radius) for each species in each shell. It also provides the object distribution into the various shells at the beginning of the simulation. After this stage, every object loses its identity and become part of the data set with mean characteristics. The launch profile is similarly obtained.

2.2. Model equations

The model uses an explicit Euler model to propagate the future states with

$$N(t + \Delta t) = N(t) + \dot{N}(t, N_i(t)) \Delta t, \quad (1)$$

where the derivative term is equal to the sum of six terms,

$$\dot{N} = \dot{C} + \dot{D} + \dot{E} + \dot{L} + \dot{M} + \dot{U}, \quad (2)$$

referring respectively to collisions, drag, explosions, launches, mitigation measures and control (ADR).

At every time step, the total population N_T is equal to the sum of all the species population N_i :

$$N_T(h,t) = \sum_h \sum_i N_i(h,t) = N_{ACP}(h,t) + N_{INP}(h,t) + N_{ROB}(h,t) + N_{MRO}(h,t) + N_{COL}(h,t) + N_{EXP}(h,t), \quad (3)$$

where h refers to the altitude shell, t to time and the subscripts ACP , INP , ROB , MRO , COL , and EXP denote respectively to the active payloads, inactive payloads, rocket bodies, MROs, explosion and collision fragments. Further details on the modelling aspects can be found in [5].

3. Reference case

In the reference case, the initial population and their mean physical characteristics are computed from 16812 objects extracted from the MASTER 2009 dataset (see Table 2 in Appendix 1). It was assumed that 90% of payload are already inactive at the beginning of the simulation, and only objects bigger than 0.1m are considered. A mean yearly launch profile is also obtained from 491 launches in the 2009-2016 timeframe (both years included, see Table 3 in Appendix 1). The simulation starts in 2009 and terminates after 200 years with an integration time step of 0.1 years. Satellites are active for eight years then become inactive. They are then removed after 25 years with a PMD compliance of 90% (and a 100% success rate). In addition, all spacecraft perform passivation, resulting in a no-explosions scenario.

The evolution of the orbital population for each species and total density are shown respectively in Figure 3, and Figure 2. The choice of represent and investigate the orbital density is driven by the fact that the orbital collision rate depends from the square of the density, and therefore peaks in the density reflects in higher collision rates (and thus more collision fragments). A visual comparison of these two physical quantities is reported in Figure 10 and Figure 11 in Appendix 2. Note that the solar cycle causes periodic ripples in the population and therefore the measured values might not assume the maximum value at the end time (see e.g. Figure 1Figure 2 and Figure 3).

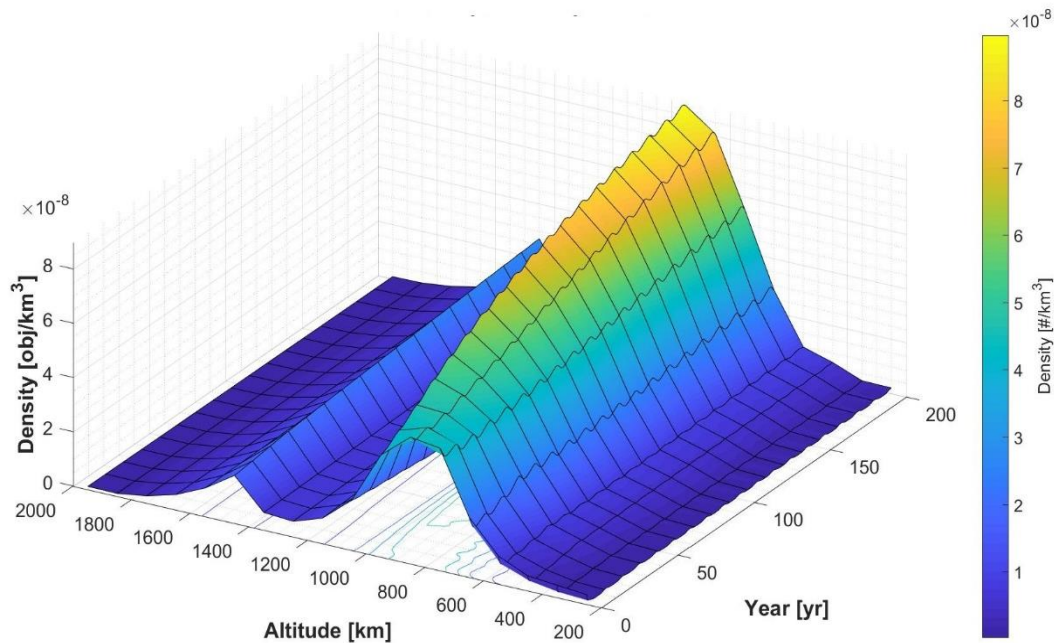


Figure 2: Evolution of the orbital density in the reference case. Values are reported at the middle point of each shell.

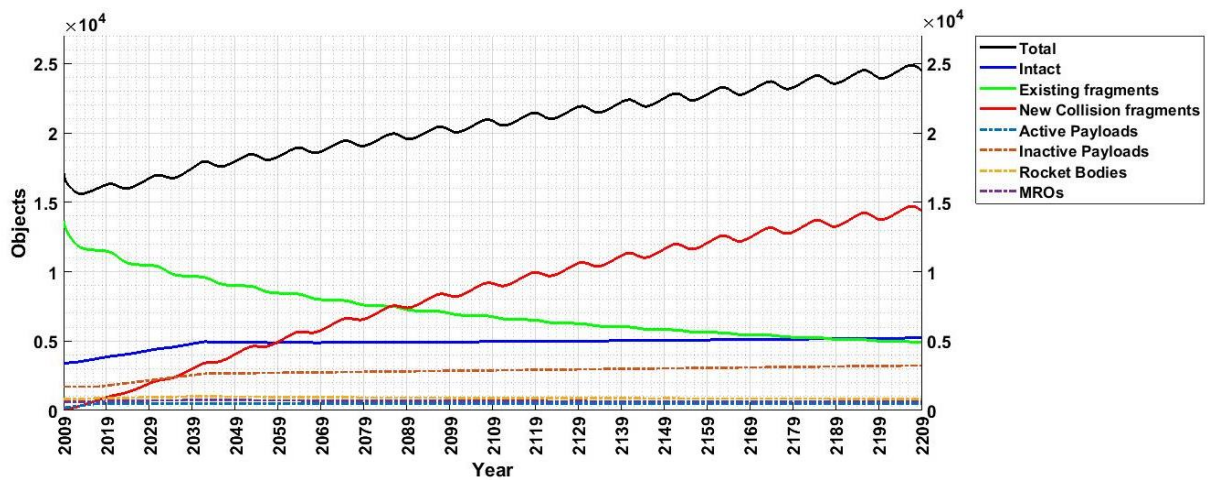


Figure 3: Evolution of total number of object in LEO for each species in the reference case.

4. Analysis and discussion

4.1. Sensitivity study on the launch rate

The first analysis performed is a sensibility study on the launch rate. Four scenarios are compared to the reference case: no-launches, half of the reference launch rate, i.e. 50% $L_0(h)$, 150% $L_0(h)$, and twice the launch rate, i.e. 200% $L_0(h)$. Figure 4 and Figure 5 illustrates respectively the evolution of the population, and the density at the end time of each scenario, while Table 1 list the numerical results. Note that due to the effect of the solar cycle, the population and density values might not assume the maximum value at the end time (see the ripples in Figure 4).

The no launch scenario is the most optimistic case, and it reveals a peak in orbital density in the 900-1000 km shell. Indeed, even if this is the only case in which the final population is lower than the original one (-12.1%, see Figure 4), the density assumes values greater than the initial one, but its peak is shifted up from 700-900 km to the 900-1000 km.

Table 1: Numerical results of the sensitivity study on the launch rate.

	Total end population	Total collisions	Maximum density at end time [# / km³]	Maximum density [# / km³]
0% $L_0(h)$, (no launches)	15 040	32.23	5.43 e-08	5.53 e-08
50% $L_0(h)$,	19 386	48.40	7.00 e-08	7.10 e-08
100% $L_0(h)$, (base case)	24 531	71.06	8.86 e-08	8.97 e-08
150% $L_0(h)$,	30 521	101.35	1.10 e-07	1.10 e-07
200% $L_0(h)$,	37 401	140.49	1.36 e-07	1.38 e-07

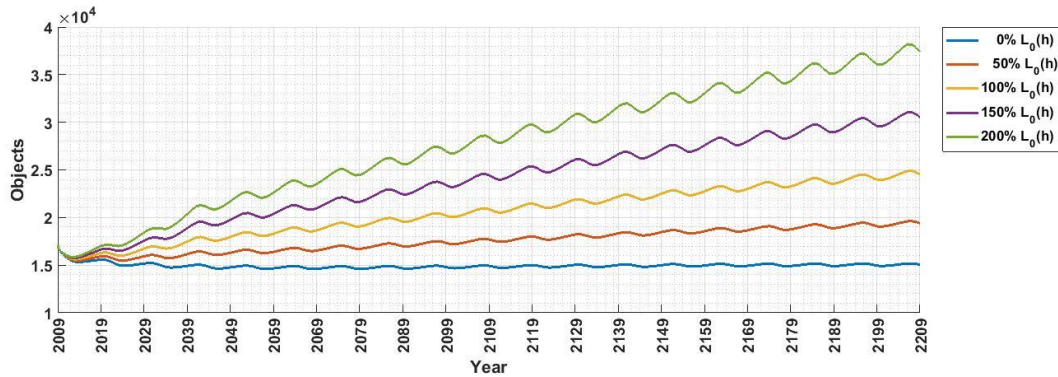


Figure 4: Comparison of total end population for various multiplier of the base launch profile $L_0(h)$.

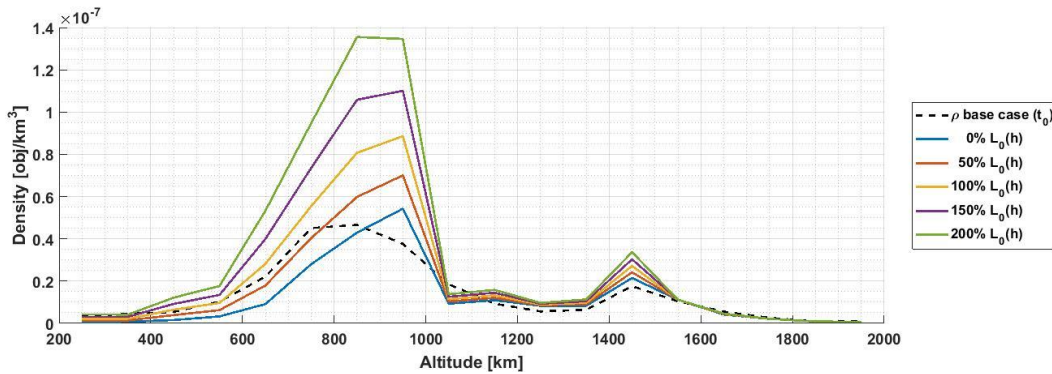


Figure 5: Comparison of orbital density at end time for various multiplier of the base launch profile $L_0(h)$.

This behaviour can also be deduced from the variation in colour in Figure 2 and is most likely due to the beneficial effect of atmospheric drag that removes more objects at lower altitudes. The same happens in the other cases, with increasing density in the same region, with the only exception for the last case (200% $L_0(h)$). In it, the density reaches its peaks in the 800-900 km region, due to the increasingly number of decaying objects from the upper shell. In the region of 1400-1500, the maximum orbital density increases with the number of launches as well, but it always assumes smaller values than the absolute peak in the lower region.

Concerning the population evolution, Table 1 suggests a linear relationship among the percentage of launches and both the end population and the total cumulative number of collisions. However, extending the simulations up to 1000% $L_0(h)$, it appears a clear non-linear trend (Figure 6) due to an increasing number of both targets and newly generated fragments that act as projectiles.

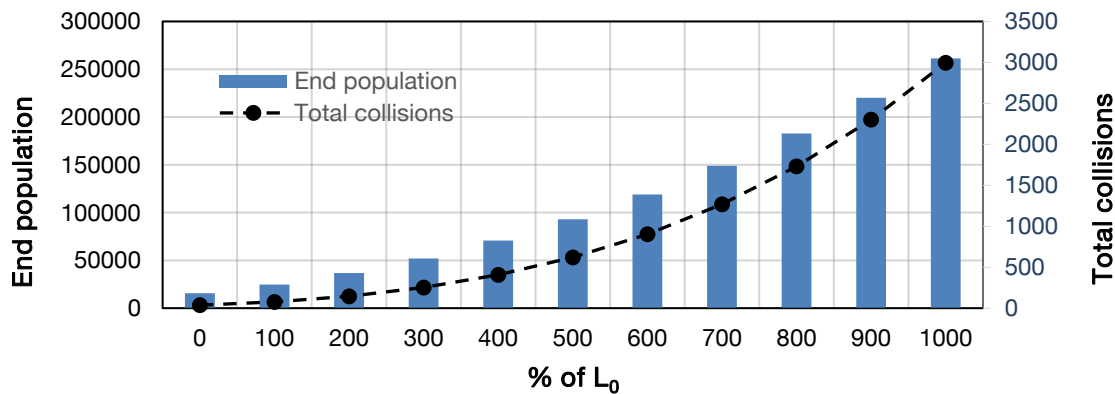


Figure 6: The end population and the total cumulative number of collisions for an extended set of simulations.

4.2. Sensitivity study on the launch profile

A second study is performed to individuate how many additional spacecraft can be supported by the environment before exceeding the threshold of $1.00 \text{ e-}7$ objects per square kilometre, equivalent to 0.1 objects in a cube with the side of 100 km. This threshold has been chosen due to its proximity to the maximum density reached at the end time in the reference case, equal to $8.97 \text{ e-}8$. Figure 7 illustrates the results, with the lower values of the curve in the two shells between 800-900 km and 900-1000 km with respectively two and four additional objects launched per year. The second lowest value (15) is reached in two contiguous shells, between 1100-1300 km. Further analysis are also carried out increasing (until the end of the simulation) by 5, 10, 15, 20 and 25 the number of launched payload per year in this second region. The evolution of the orbital population and the density in 1100-1200 km are shown in Figure 8 and Figure 9. Results in 1200-1300 km are very similar and are not reported here.

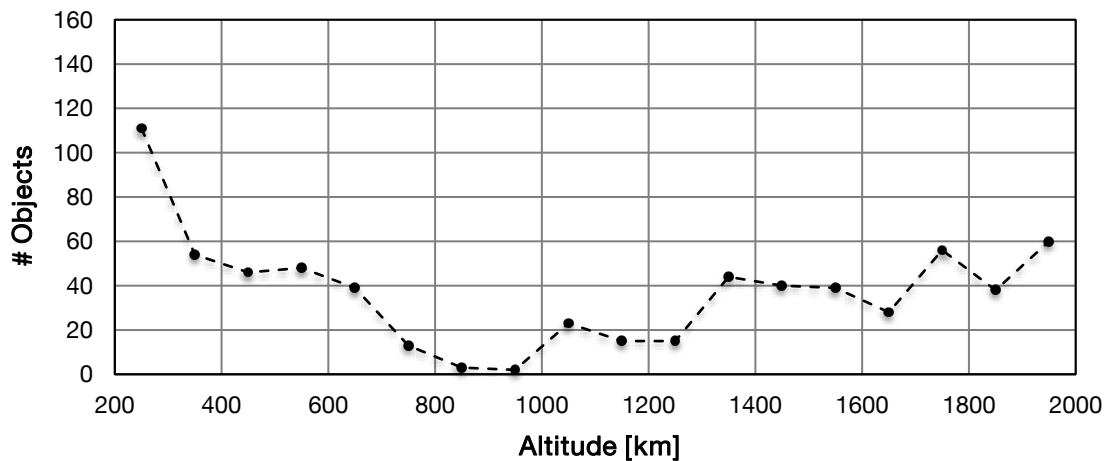


Figure 7: Number of additional launched payloads in each shell to reach the density of $1\text{e-}7$ objects per square kilometre.

As shown by the dotted line in Figure 9, today's more crowded region are between 700-1000 km and 1400-1500. However, the regions that require the lower additional number of launches to reach the selected threshold are between 800-1000 km and 1100-1300 km (Figure 7). For altitudes less than 700 km the natural drag prevent the build-up of the population even if more collisions may occurs at these low altitudes during the simulation. Above 1300 km, the values range between 28 and 60. At these altitudes the atmospheric drag is negligible, while the increase in the shell volume (the upper shell is 1.58 times the lower one) helps to decrease the density and the collision risk and therefore slightly increases the slope of the curve. The resulting differences are therefore due only to the difference in the assumed mean values of the physical characteristics, especially of the radius that determines the collision rate.

In the region of 1100-1300 km, the beneficial effects of the atmospheric drag are very weak, and both the population and the orbital density increases more than linearly with the number of additional payloads (Figure 8 and Figure 9). The interest in this region has been revealed by several private companies that proposes to launch constellation in order to provide a global internet coverage. The presented results are valid under the hypothesis that additional payload have the same mean characteristics of the past 8-yr launches (with a mean radius and mass are respectively 1.09 m and 1283 kg), while the proposed constellation are formed by smaller and lighter spaceft (about 150-200 kg and a radius smaller than 0.5 m).

Conversely to the work presented in [3], where the additional objects forms a constellation active only for 50 years and the negative effect were limited in time, in our study (where the launch rate is constant until the end of the simulation) the effects are permanent in this region and increases with time and number of additional launches.

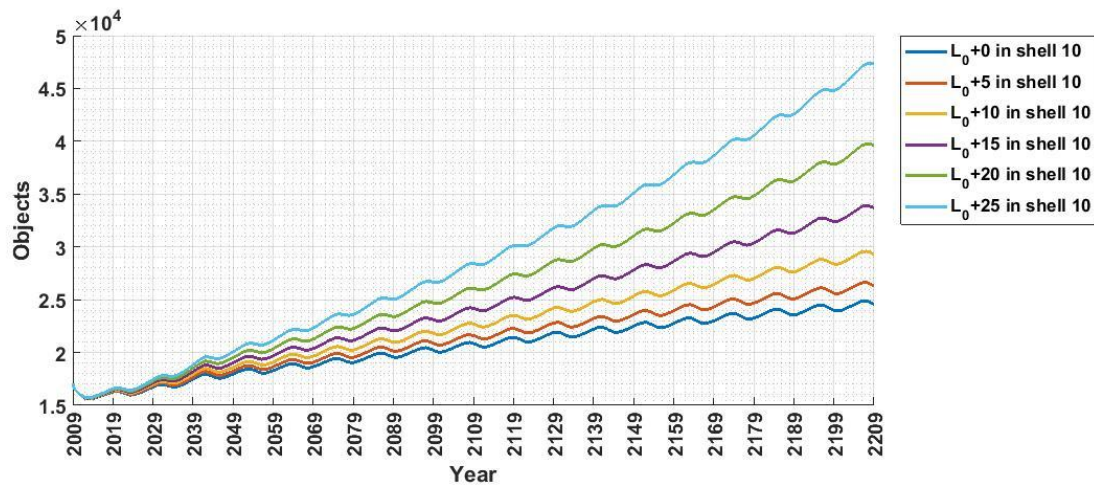


Figure 8: Evolution of population when increasing by 0, 5, 10, 15, 20 and 25 the payload launched per year between 1100 and 1200 km.

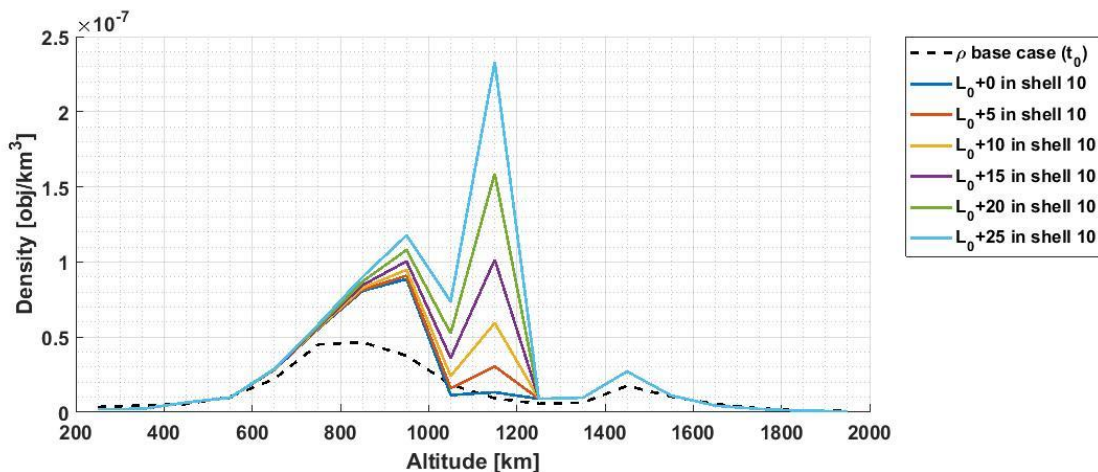


Figure 9: Evolution of density at end time when increasing by 0, 5, 10, 15, 20 and 25 the payload launched per year between 1100 and 1200 km

5. Conclusions

Several sensitivity analysis on the launch rate and profile were performed using the MISSD model. The results suggest that two regions are particularly critic in LEO. The first one lies at 800-1000 km, where today population causes the increase in future orbital density. Only in the no-launch case, thanks to the positive action of natural drag, the lowest part of this region assumes value smaller than the initial ones. The second region extends from 1100 to 1300 km. Here the initial population is low but the effect of drag is negligible. Therefore, any additional object that reaches orbit in this region contribute to the build-up of the orbital population, reaching with only 15 more spacecraft per year, the same orbital density of the lower region at end time in the reference case. Even if the simulated scenario differs in number and physical characteristics from proposed mega constellations, these results can be taken as a warning of the criticity of this second region.

Acknowledgements

The Doctoral Training Partnership funded part of this research through the Engineering and Physical Sciences Research Council (EPSRC) Grant EP/M50662X/1. ESA Space Debris Office provided data on the orbital population and launch traffic.

References

- [1] J.C. Dolado-Perez, C. Pardini, L. Anselmo, Review of the uncertainty sources affecting the long-term predictions of space debris evolutionary models, *Acta Astronaut.* 113 (2015) 51–65. doi:10.1016/j.actaastro.2015.03.033.
- [2] J. Radtke, C. Kebschull, E. Stoll, Interactions of the space debris environment with mega constellations - Using the example of the OneWeb constellation, *Acta Astronaut.* 131 (2017) 55–68. doi:10.1016/j.actaastro.2016.11.021.
- [3] B. Bastida Virgili, J.C. Dolado, H.G. Lewis, J. Radtke, H. Krag, B. Revelin, C. Cazaux, C. Colombo, R. Crowther, M. Metz, Risk to space sustainability from large constellations of satellites, *Acta Astronaut.* 126 (2016) 154–162. doi:10.1016/j.actaastro.2016.03.034.
- [4] G.L. Somma, H.G. Lewis, C. Colombo, Adaptive remediation of the space debris environment using feedback control, in: *67th Int. Astronaut. Congr.*, Guadalajara, Mexico, 2016: pp. 1–11. <https://eprints.soton.ac.uk/403265/>.
- [5] G.L. Somma, C. Colombo, H.G. Lewis, A Statistical LEO Model to Investigate Adaptable Debris Control Strategies, in: *2017 - 7th Eur. Conf. Sp. Debris*, Darmstadt, Germany, 2017: pp. 1–12.
- [6] P.H. Krisko, N.L. Johnson, J.N. Opiela, Evolve 4.0 Orbital Debris Mitigation Studies, *Adv. Sp. Res.* 28 (2001) 1385–1390.
- [7] P.H. Krisko, Proper Implementation of the 1998 NASA Breakup Model, *Orbital Debris Q. News.* 15 (2011) 4–5.
- [8] D.G. King-Hele, *Satellite Orbits in an Atmosphere: Theory and Application*, Glasgow Blackie, Glasgow, 1987.
- [9] D.A. Vallado, *Fundamentals of Astrodynamics and Applications*, 4th ed., Microcosm Press and Springer, Hawthorne, CA, 2013.

Appendix 1 – Additional tables

Table 2: The initial population in the base reference case.

Altitude [km]	Total Payloads	Rocket Bodies	MROs	Collision Fragments	Explosion Fragments	Total [# /yr]
200-300	3	4	9	12	163	191
300-400	25	9	1	9	208	252
400-500	55	27	15	11	206	314
500-600	104	56	34	16	399	609
600-700	165	98	73	49	963	1348
700-800	300	105	110	110	2205	2830
800-900	158	98	62	118	2570	3006
900-1000	261	198	142	100	1795	2496
1000-1100	50	42	79	54	1034	1259
1100-1200	80	41	44	25	462	652
1200-1300	9	8	6	16	368	407
1300-1400	51	19	13	22	369	474
1400-1500	532	51	24	36	687	1330
1500-1600	54	59	15	34	651	813
1600-1700	16	10	5	25	385	441
1700-1800	3	6	3	11	189	212
1800-1900	2	0	1	5	76	84
1900-2000	1	4	2	3	84	94
Total	1869	835	638	656	12814	16812

Table 3: The number of launches per year in the reference case.

Altitude [km]	Intact Payloads [#/yr]	Rocket Bodies [#/yr]	MROs [#/yr]	Total launches [#/yr]
200-300	1.250	0.375	0.125	1.750
300-400	1.000	0.250	0.250	1.500
400-500	4.500	2.125	1.250	7.875
500-600	4.750	3.000	1.125	8.875
600-700	12.375	2.375	2.625	17.375
700-800	4.870	1.375	1.125	7.375
800-900	2.875	1.125	0.875	4.875
900-1000	2.625	1.500	0.625	4.750
1000-1100	0.375	0.375	1.125	1.875
1100-1200	0.375	0.250	0.750	1.375
1200-1300	0.000	0.125	0.000	0.125
1300-1400	0.250	0.125	0.000	0.375
1400-1500	2.250	0.625	0.125	3.000
1500-1600	0.000	0.000	0.000	0.000
1600-1700	0.125	0.125	0.000	0.250
1700-1800	0.000	0.000	0.000	0.000
1800-1900	0.000	0.000	0.000	0.000
1900-2000	0.000	0.000	0.000	0.000
Total	37.625	13.750	10	61.375

Appendix 2 – Additional figures

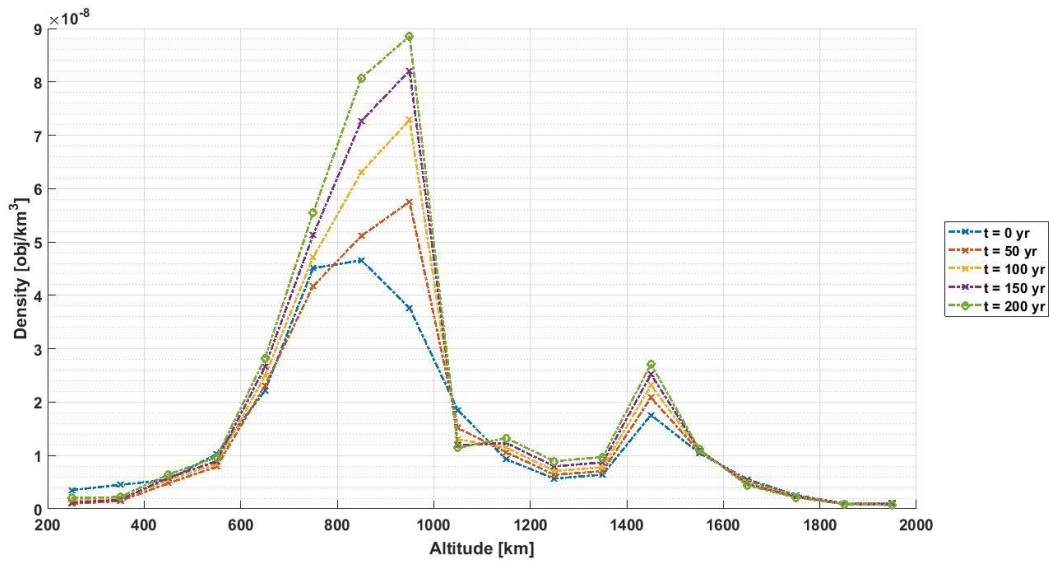


Figure 10: Evolution of the orbital density in the reference case. Values are reported at the middle point of each shell.

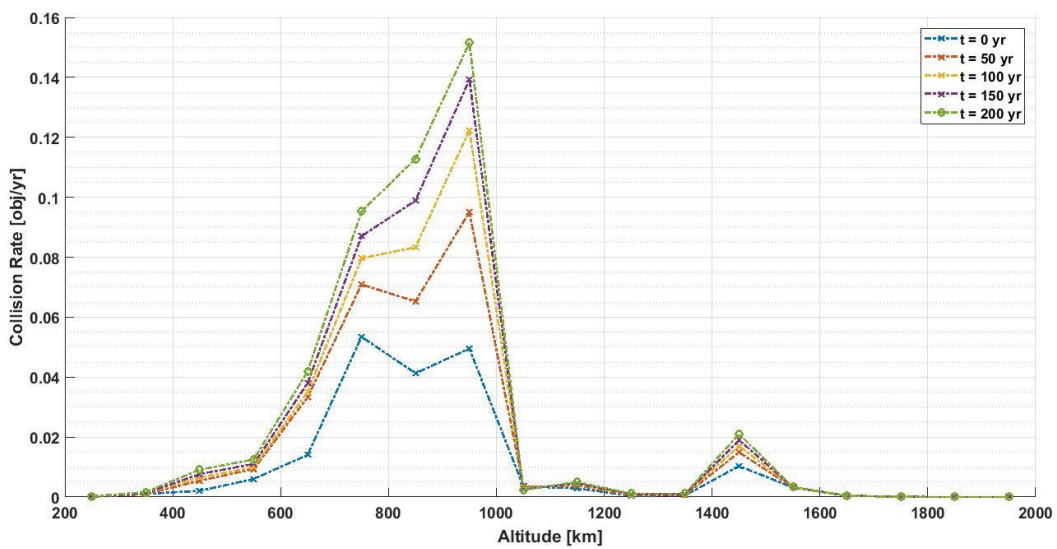


Figure 11: Evolution of the collision rate and orbital density in the reference case. Values are reported at the middle point of each shell.